ELECTROREFLECTANCE OF DISORDERED GERMANIUM FILMS

H. Piller,* B. O. Seraphin,† K. Markel, and J. E. Fischer
Michelson Laboratory, China Lake, California 93555
(Received 25 August 1969)

The transition from the crystalline to the amorphous state has been studied in germanium thin films by observing the electroreflectance spectra related to critical points at Γ ($E_0, E_0+\Delta_0$), along the Λ direction ($E_1, E_1+\Delta_1$), and at areas with Δ and Σ symmetry (E_2). A small shift of E_0 to lower energy with increasing disorder in the crystalline state, and weak structure in the amorphous state, have been observed. The spectral positions of E_1,$E_1+\Delta_1$ and E_2 do not change with disorder in the crystalline state but these responses are completely absent in the amorphous state.

Increasing attention has recently been paid to the correlation between the electronic structure of a solid and the degree of long-range order in its lattice.[1,2] Many experimental results suggest that the amorphous state retains a residual energy-band structure.[3-5] However, little is known about its detailed features, or how it evolves from the band structure of the crystalline state as disorder is gradually introduced.

We report in this Letter the electroreflectance spectra of a series of germanium films deposited onto substrates of various temperatures. In such a set of samples, the long-range order is systematically reduced towards cooler substrates, and a transition from the polycrystalline to the amorphous state is passed. Static reflectance spectra, which for each photon energy monitor the sum of all possible transitions in the entire Brillouin zone, drastically lose the sharpness of their spectral features as the completely disordered state is approached.[3,5] In electroreflectance, only transitions near localized, structure-sensitive discontinuities of the electronic density-of-states function respond to the electric-field perturbation.[6] In contrast to "integral" properties, electroreflectance is therefore expected to monitor more sensitively the gradual weakening of order-dependent features in the band structure as the long-range order is reduced.

In a set of evaporated germanium films, the transition from "polycrystalline" to "amorphous" occurs at a substrate temperature $T_s{}^t$ that depends upon evaporation rate, vacuum conditions, and substrate material. Accordingly, a wide range of values $T_s{}^t$ extending from 100°C to slightly below 400°C has been reported. In this study we closely controlled the evaporation conditions, so that mainly the substrate temperature T_s, varied in steps of 25°C over the range $100 \leq T_s \leq 500$°C, determined the crystalline order of the film. Controlled by an acoustic thickness monitor (Sloan), all samples of the set are 2400 $\pm$ 200 Å thick, prepared at a growth rate of 7-10 Å/sec in a vacuum of $(4\text{-}7)\times10^{-7}$ Torr. Three different types of substrates were coated for each temperature T_s. Two consisted of single-crystal germanium, polished to a final abrasive diameter of 1 μ, one of which subsequently was coated with an opaque layer of aluminum. The film on the third substrate, a quartz flat, served for measurements of the electron diffraction pattern and of the space-charge capacitance. The electroreflectance spectra were recorded on the films deposited on the germanium substrates, thereby keeping mechanical strain to a minimum. In separate runs we made sure that reflections from the substrate-film interface did not contribute to the electroreflectance response.

The electron-beam diffraction results indicate a transition temperature $175 < T_s{}^t < 200$°C for our set of samples, near which the sharp ring pattern is abruptly blurred. In the same temperature range we observe the changes in the spectra reported below. The polycrystalline films above the transition displayed a pattern indicative of a predominantly (110) orientation.

The spectra were recorded in the dry-sandwich configuration[6] consisting of the sample film, a 200-Å thick Al_2O_3 dielectric layer, and a semitransparent Ni field electrode. Field strengths of 10^6 V/cm or more can be applied across this sample sandwich. It must be assured, however, that the space-charge layer in which the response originates can be modulated by the external field throughout the range of disorder. No conclusions with respect to the band structure should be drawn from a disappearance of some structure in the amorphous state, for instance, before the persistance of space-charge modulation in this state has been established. We have therefore measured the modulation of the surface capacitance on the entire set of samples and demonstrated that the potential barrier follows the external modulation. This is a new result in itself

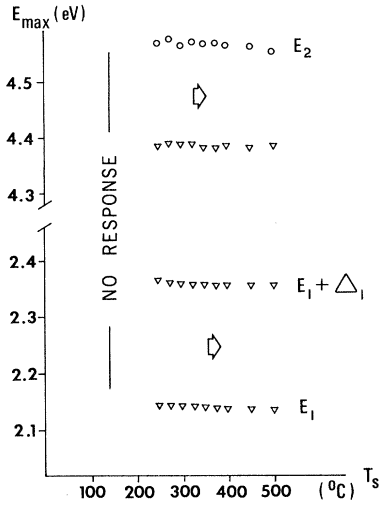

FIG. 1. Spectral position E_{max} of four peaks (open circles, positive; inverted triangles, negative) in the electroreflectance of germanium films deposited onto germanium substrates of various temperatures T_S. Arrows indicate the direction of increase of the response.

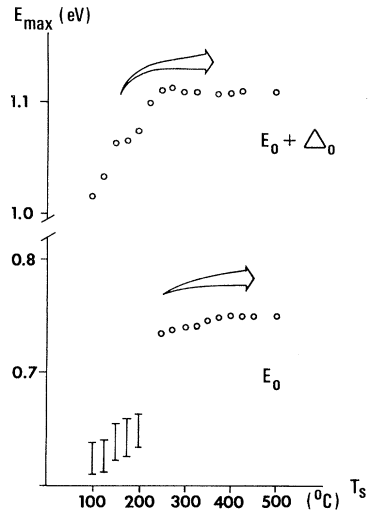

FIG. 2. Same as Fig. 1, but for the fundamental edge E_0 and its spin-orbit–split companion $E_0+\Delta_0$. Bars below 200°C indicate approximate position of weak structure.

and will be reported in a separate paper.[7]

Erroneous spectra are observed near photon energies for which the interferometer that the system of thin films represents is optically matched. Near the fundamental edge the light penetrates sufficiently far for multiple internal reflections to occur, and the ratio of electroabsorption to electroreflectance in their fractional contribution to the observed signal is drastically changed. Our sample thickness of 2400 Å places the resonances of the optical cavity outside the spectral ranges of interest.

We used an experimental setup frequently described before,[6] and covered at room temperature the spectral range from 0.6 to 4.6 eV. Four groups of structure are observed in this range which, in a notation introduced by Cardona for static reflectance spectra,[8] will be called E_0 (0.6-0.8 eV), $E_0+\Delta_0$ (0.9-1.1 eV), $E_1, E_1+\Delta_1$ (2.1-2.3 eV), and E_2 (4.3-4.5 eV). The first two are correlated to the fundamental edge and its spin-orbit–split companion; the third, a spin-orbit–split doublet, to a critical point along the Λ direction of the Brillouin zone; and the fourth is assigned to a mixture of contributions from areas with Δ and Σ symmetry.

Proceeding through the sample set in the direction of decreasing substrate temperature and therefore increasing disorder, we made the following observations, as summarized in Figs. 1 and 2.

(1) Within the experimental error of ±5 meV, the spectral position of the $E_1, E_1+\Delta_1$ and the E_2 structures does not change over the range of substrate temperatures 200 to 500°C (Fig. 1). The line shape, in particular the relative linewidth of the structures, also remains unchanged.

(2) The size of an electroreflectance response is a notoriously poor parameter, affected by even slight changes in the formation of the space-charge layer. However, in spite of fluctuations among the set of samples, the sizes of the $E_1, E_1+\Delta_1$ and E_2 structures decrease towards lower substrate temperatures, as indicated by arrows in Fig. 1. The size drops more steeply between 300 and 200°C, and no signal could be obtained below $T_S = 200$°C, although modulation and sensitivity were stretched to the limit. All structures stay sharp until they disappear, their relative linewidth apparently unaffected by the increasing degree of disorder.

(3) As shown in Fig. 2, the spectral position of the $E_0+\Delta_0$ stays constant in the range $250 \leq T_S \leq 500$°C. As the transition temperature is approached from above, the spectral position shifts gradually to smaller photon energies, ending for a sample temperature of 100°C at a value 0.1 eV below its crystalline value.

The size of this structure, fluctuations notwithstanding, decreases steadily over the entire range. Note that it does not disappear below the transition temperature, but can clearly be observed even in the highly disordered state. The linewidth increases slightly below $T_S = 200$°C.

(4) Unique among the four structures recorded, the spectral position of E_0 shifts over the entire range of substrate temperatures. Although small, the red shift between 500 and 250°C is well beyond experimental error.

After decreasing steadily in size, the line shape of E_0 changes drastically at $T_s = 200$°C. Below this temperature, a very weak and broad response is observed at photon energies 0.1 to 0.2 eV smaller than the response in the crystalline state. Although present beyond doubt, the structure is marginal even at large values of modulation, sensitivity, and spectral resolution. Any interpretation must allow for wide margins in size, line shape, and spectral position.

(5) The line shapes of the three higher structures do not change throughout the range $250 \leq T_s \leq 500$°C. The fundamental structure E_0, however, is different for films of n-type and p-type character. Films of small n-type thermoelectric response display a single peak. Films responding strongly p type in the thermoelectric measurements exhibit an additional peak of equal strength, located at larger photon energy. It is tempting to correlate these two peaks observed in p-type samples with transitions from light- and heavy-hole states in the valence band, as observed in the interband absorption of other semiconductors.[9] A speculative interpretation could even recognize a doublet nature in the weak and poorly resolved structure below $T_s = 200$°C, taking into account the known p-type character of amorphous films. Although well established in p-type crystalline semiconductors, such an interpretation will deserve confidence only after considerably more experimental information is available from disordered systems.

Our theoretical understanding of the electronic structure of disordered solids is insufficient to interpret our results in terms of a specific band model. We can condense our results, however, into the following:

(a) The electronic structure in areas contributing to $E_1, E_1 + \Delta_1$ and E_2 is virtually unaffected above the transition temperature $T_s{}^t$. The gradual reduction in size of these structures is not accompanied by broadening, and might be due to the order-dependent formation of the space-charge layer. On the amorphous side of the transition, all these structures disappear, suggesting a drastic impact on the critical-point character. This is in agreement with measurements of static reflectance and photoemission by Donovan and co-workers[5,10] on a similar set of films. With a diffraction-determined transition temperature near 200°C, structure in both reflectance and photoemission associated with crystal symmetry disappeared below 225-250°C, being well defined above 300°C substrate temperature. No shifting of peak positions with substrate temperature was observed, nor did any particular peak appear prior to any other.

(b) The fundamental structure E_0 reflects the increasing degree of disorder in a systematic shift of its spectral position. Unlike size or line shape of an electroreflectance structure, its spectral position is a significant parameter. The red shift with decreasing substrate temperature documents the increase of disorder even in a range in which for all other purposes the samples can be considered polycrystalline. It establishes a definition for the order of film that we could rely on in our sample preparation. Conditions of evaporation outside the control range manifested themselves in shifts of the spectral position into the proper direction, rendering a sample more "amorphous" or more "polycrystalline."

Although extremely weak and ill defined, some structure is still observed below the transition temperature. Its position at photon energies typically 0.2 eV below the crystalline value agrees well with measurements of Donovan and co-workers,[10] who find a sharp absorption edge near this photon energy on films deposited at room temperature. Speculating on the strongly p-type character of amorphous films, the broad and weak double structure can be correlated with the transitions from heavy- and light-hole bands (or their equivalents in the perturbed band structure) familiar from optical measurements on other p-type semiconductors.[9]

(c) The spin-orbit–split transition correlated with $E_0 + \Delta_0$ provides a better defined replica of the band structure near $k = 0$ over the range of disorder. Above $T_s{}^t$, the structure does not follow the slight red shift of the E_0 structure, indicating in a small effective increase in the spin-orbit splitting Δ_0. Near the transition temperature, the structure shifts strongly to smaller photon energies, and can still be observed in the highly disordered state. The interior of the valence band, from which this transition starts, is apparently less affected by the loss of the long-range order. Since the fundamental structure reacts so differently from its spin-orbit–split companion, we can conclude that the top of the valence band is more strongly affected by the loss

of long-range order than the bottom of the conduction band which both transitions share as their final state. Although clearly seen on polycrystalline films, no evidence of a spin-orbit–split valence band has so far been reported in absorption of amorphous films.

The authors would like to thank E. Bauer and J. H. Dancy for the electron diffraction measurements and acknowledge valuable discussions with T. M. Donovan.

*Present address: Department of Physics, Louisiana State University, Baton Rouge, La. 70803.

†Temporary address: Physics Institute I, Technical University of Denmark, 2800 Lyngby, Denmark.

[1]N. F. Mott, Contemp. Phys. 10, 125 (1969).

[2]F. Herman and J. P. Van Dyke, Phys. Rev. Letters 21, 1575 (1968).

[3]J. Tauc, Science 158, 1543 (1967).

[4]J. Stuke, Phys. Status Solidi 6, 441 (1964).

[5]T. M. Donovan and W. E. Spicer, Phys. Rev. Letters 21, 1572 (1968).

[6]B. O. Seraphin, in "Semiconductors and Semimetals," edited by R. K. Willardson and A. C. Beer (Academic Press, Inc., New York, to be published), Vol. VI, "Electroreflectance."

[7]K. E. Markel, B. O. Seraphin, and H. Piller, to be published.

[8]M. Cardona, J. Appl. Phys. 32, 2151 (1961).

[9]O. Madelung, Physics of III-V Compounds (John Wiley & Sons, Inc., New York, 1961).

[10]T. M. Donovan, W. E. Spicer, and J. M. Bennett, Phys. Rev. Letters 22, 1058 (1969).

THEORY OF DEFECTS IN QUANTUM CRYSTALS*

C. M. Varma

Bell Telephone Laboratories, Murray Hill, New Jersey 07974, and
School of Physics, University of Minnesota, Minneapolis, Minnesota 55455

(Received 14 July 1969)

We generalize the existing theory of isotope defects by a variational method to be applicable to quantum crystals, where renormalization effects are crucial, and compare the results thus obtained with experiments.

The effect of isotopic defects on the properties of quantum crystals is very striking. For example, there is experimental evidence that the defect contribution to the thermal resistivity of solid mixtures of ^{3}He and ^{4}He is larger, and its concentration dependence stronger,[1-3] than expected from the theory of defects in classical crystals; the exchange frequency in solid ^{3}He for sites around the ^{4}He impurity has been deduced by some NMR workers to be appreciably larger[4] than in pure crystals; solid mixtures have measurable phase-separation times[5]; and there are large effects on spin-lattice relaxation times[4] in solid ^{3}He for ^{4}He concentration as small as 10^{-5}. Here we point out why the theory of defects in classical crystals is inapplicable to our problem, generalize the theory to be meaningful for quantum crystals, and compare the results with experiment.

First we briefly review the theory of defects in classical crystals.[6] Let the pure crystal be composed of N particles of mass m arranged in a Bravais lattice and interacting with each other with harmonic force constants $P_{\alpha\beta}(l,l')$ (l,l' label the sites and α,β the Cartesian directions). In the presence of defects, the $3N$ equations of motion for the lattice displacements $u_\alpha(l)$ are

$$m\omega^2 u_\alpha(l)+\sum_{\beta l'}P_{\alpha\beta}(l,l')u_\beta(l')=\sum_{\beta l'}D_{\alpha\beta}(l,l')u_\beta(l'), \tag{1}$$

where

$$D_{\alpha\beta}(l,l')=-\Delta m(l)\omega^2\delta_{\alpha\beta}\delta(l,l')+\Delta P_{\alpha\beta}(l,l'), \tag{2}$$

and $\Delta m(l)$, $\Delta P_{\alpha\beta}(l,l')$ are deviations from perfection, and ω are frequencies to be determined. Normal coordinates $q(\nu)$ are now introduced:

$$u_\alpha(l)=\sum_\nu T_\alpha(\nu,l)q(\nu), \tag{3}$$

where ν labels the $3N$ new coordinates in place of the wave vector $\vec{k}$ and polarization index λ for the perfect crystal. The eigenvectors $T_\alpha(\nu,l)$ satisfy

$$-\omega_\nu^2 m T_\alpha(\nu,l)+\sum_{\beta,l'}P_{\alpha\beta}(l,l')T_\beta(\nu,l')=\sum_{\beta l'}D_{\alpha\beta}(l,l')T_\beta(\nu,l'), \tag{4}$$